

## VIABILITY OF USING WIND TURBINES FOR ELECTRICITY GENERATION IN ELECTRIC VEHICLES

Francisco Rubio<sup>1</sup>, Carlos Llopis-Albert<sup>1</sup>

<sup>1</sup>Centro de Investigación en Ingeniería Mecánica (CIIM), Universitat Politècnica de València,  
Camino de Vera s/n, 46022 Valencia, Spain

Emails: frubio@mcm.upv.es, cllopisa@upvnet.upv.es

Received: 2019-02-08; Accepted: 2019-04-25

### Abstract

This paper presents a feasibility study of applying a fluid energy recovery system by means of wind turbines for charging batteries of electric vehicles. This is because the main disadvantage of electric vehicles with regard to conventional fuel automobiles is the scarce capacity of storing sufficient energy to run long distances. This can be carried out by recovering a percentage of the energy used to overcome the aerodynamic drag of the vehicle. This work analysis different case studies, with different driving modes, to quantify the theoretical energy recovered from the vehicle aerodynamics. Results have shown the theoretical possibility to implement this technology in actual electric vehicles.

### Keywords

Electric vehicles, wind turbines, energy recovery, aerodynamics, battery charging.

## 1. Introduction.

A wind turbine can operate as an energy recovery system (ERS) similar to the brakes, i.e., regenerative braking (Valero et al., 2017). When a car changes its speed in any sense or direction, its amount of energy varies (Bangi et al., 2017; Ferdous et al., 2011). When it loses speed, that energy tends to dissipate. Traditionally the dissipated energy has been wasted. That is, the kinetic energy of the vehicle is transformed into heat during braking. In recent years, due to greater awareness of society about environmental issues, pollution and climate change, there is a great interest in developing energy recovery systems. One of the best known is the regenerative braking systems, which is based on the kinetic energy recovery system (KERS) during vehicle braking. This allows reductions in consumption (efficiency increases) of up to 45%.

In this article we analyze the feasibility of using a wind turbine as an energy recovery system, quantifying the savings that can be made in its two possible uses: as an energy recovery system and as a system using the aerodynamic drag, i.e., the force acting opposite to the relative motion of the vehicle moving with respect to the surrounding air (Wen-Long Yao and Chiu., 2015; Valero et al., 2019). The recovered energy can be used for electric vehicle charging, thus reducing costs (Llopis-Albert et al., 2015; 2018; 2019). This can play a major role since electric vehicles sales have increased significantly during last years (Zheng et al., 2018). In addition, a procedure for shape optimization of the wind turbine should be performed to increase the energy recovered (Llopis-Albert et al., 2018a). There are many optimization procedures in the literature in different research areas (Rubio et al., 2015; 2016; 2019; Llopis-Albert and Pulido-Velazquez, 2015; Llopis-Albert and Capilla, 2010; Llopis-Albert et al., 2016).

## 2. Case studies.

This work uses a wind turbine with a horizontal axis and 50 cm of diameter installed in the frontal part of a vehicle. This vehicle will be subjected to three different driving scenarios that will be characterized by speeds, accelerations and time of circulation.

**2.1 First scenario:** corresponds to a Worldwide Harmonized Vehicle Test Procedure (WLTP). In this cycle, the vehicle undergoes a 30-minute ride with certain characteristics of speeds and accelerations and routes (Table 1). Accelerations from 0 to 50 km/h must be made between 5 and 10 seconds and a distance of 27 km is travelled. It is intended to measure the power used to get the vehicle to move under the stipulated driving conditions.

More specifically, the WLTP cycle lasts 30 minutes and consists of 4 phases:

- Phase 1: low speed (589 s-9.18 min); maximum velocity ( $V_{max}$ ) = 56.5 km/h.
- Phase 2: average speed (433 s-7.22 min);  $V$  maximum velocity ( $V_{max}$ ) = 76.6 km/h.
- Phase 3: high speed (455 s-7.58 min); maximum velocity ( $V_{max}$ ) = 97.4 km/h.
- Phase 4: very high speed (323 s-5.38 min); maximum velocity ( $V_{max}$ ) = 131.3 km/h.

Different driving modes (Rubio et al., 2019) are simulated covering city (urban), secondary road, autonomous or national road and freeway. In the freeway the maximum speed will be 131 km/h and the average protocol speed of 46.5 km/h.

**Table 1:** Circulation characteristics for scenario 1 (WLTP cycle).  
V: velocity, A: acceleration

Phase	Time (s)	Stop (s)	Distance (m)	% stop	V_max (km/h)	A_min (m/s <sup>2</sup> )	A_max (m/s <sup>2</sup> )
Low	589	156	3095	26.5	56.5	-1.47	1.47
Medium	433	48	4756	11.1	76.6	-1.49	1.57
High	455	31	7158	6.8	97.4	-1.49	1.58
Super high	323	7	8254	2.2	131.3	-1.21	1.03
Total	1800	242	23262				

**2.2 Second scenario:** It corresponds to a purely urban driving (in city) with the following characteristics:

Cycle time: 20.25 min.

Time in circulation: 15.55 min

Stop time: 4.7 min

Distance travelled: 8.84 km

Maximum speed: 50 km/h

During the journey there are ups, downs, accelerations, decelerations and stops.

**2.3 Third scenario:** It corresponds to an interurban driving (highway) with the following characteristics:

Cycle time: 1.7 h

Time in circulation: 1.7 h

Stop time: 0 min

Distance travelled: 198.79 km

Maximum speed: 120 km/h

During the journey we have considered ups, downs, accelerations and decelerations.

### 3. Driving modes and acting forces.

Table 2 shows the driving modes of the vehicle and the braking or driving force that must be provided for the vehicle to move under the conditions set by the corresponding driving mode.

**Table 2:** Driving modes

#### Case 1: Acceleration in plain



$$F_m = -F_i + F_r + F_a + F_w$$

#### Case 2: Deceleration in plain



$$F_{fren} = -F_i + F_r + F_a + F_w$$

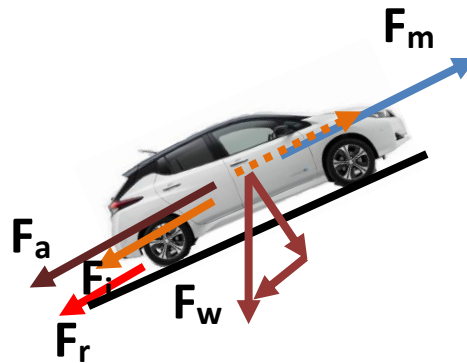
#### Case 3: Constant velocity



$$F_m = -F_i + F_r + F_a + F_w$$

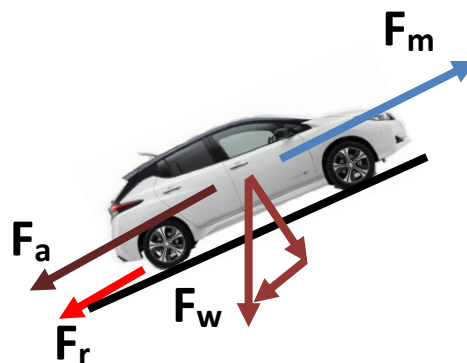
**Table 2:** Driving modes (continued)

**Case 4: Acceleration upwards**



$$F_m = -F_i + F_r + F_a + F_w$$

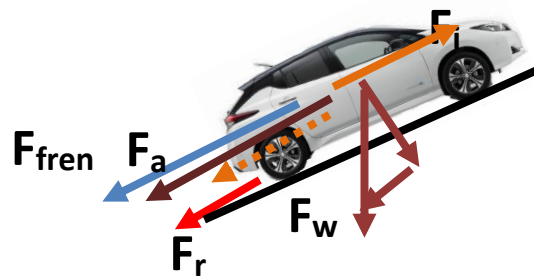
**Case 5: Constant velocity upwards**



$$F_m = -F_i + F_r + F_a + F_w$$

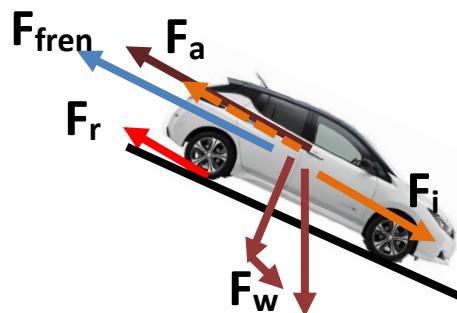
**Table 2:** Driving modes (continued)

**Case 6: Deceleration upwards**



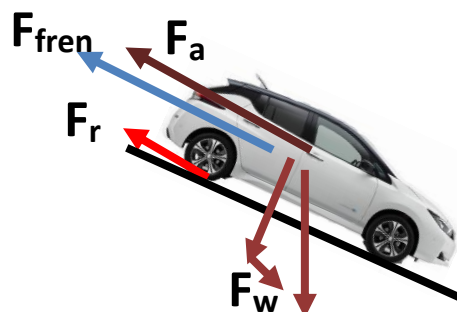
$$F_{fren} = -F_i + F_r + F_a + F_w$$

**Case 7: Deceleration downwards**



$$F_{fren} = -F_i - F_w + F_r + F_a$$

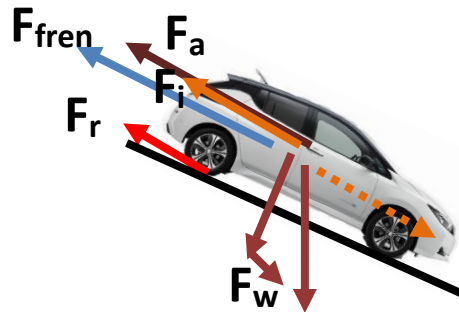
**Case 8: Constant velocity downwards**



$$F_{fren} = -F_i - F_w + F_r + F_a$$

**Table 2:** Driving modes (continued)

**Case 9: Acceleration downwards**



$$F_{fren} = -F_i - F_w + F_r + F_a$$

The forces considered in the conduction of the automobile are:

- $F_m$  = driving force  $F$
- $F_i$  = inertia force
- $F_r$  = rolling force
- $F_a$  = dragging force
- $F_w$  = weight
- $F_{fren}$  = braking force

The power is calculated as follows:  $P = F_{m/fren} \cdot v$ .

**4. Results. Analysis of the consumed power**

The most important vehicle characteristics and the set of parameters used in the calculation of the different forces that act on it are presented in Table 3:



**Table 3:** Parameters

<b>A</b>	2,2	m <sup>2</sup>
<b>C</b>	0,32	-
<b>m</b>	1000	kg
<b>θ</b>	0	rad
<b>ρ</b>	1,225	kg/m <sup>3</sup>
<b>g</b>	9,81	m/s <sup>2</sup>

Where **A** is the front area of the vehicle; **C**: drag coefficient; **m**: mass of the vehicle; **θ**: angle of the ramp up or down; **ρ**: air density; **g**: acceleration of gravity;

For the calculation of the rolling force, the coefficient of rolling resistance is  $f_r = 0.01 \cdot \left(1 + \frac{V}{160}\right)$ , where the velocity (V) is given in km/h.

The value of the air density has been considered  $\rho = 1.25 \text{ kg/m}^3$  at atmospheric pressure and at 15 °C and  $\theta$  corresponds to the slope of the up and down ramps. The acceleration in each section is calculated using the equations of the uniformly accelerated rectilinear movement taking into account the initial, final speed and the elapsed time. The values obtained for the different scenarios allows to determine the motor power and braking power required to drive according to the circulation characteristics described for each scenario. In these scenarios, the different driving modes described in Table 2 have been taken into account. The driving power affects the energy consumption of the vehicle to maintain the desired circulation characteristics. The braking power corresponds to the power dissipated in the form of heat to maintain the vehicle speed. It appears when the brakes of the motion regulation intervene.

The dissipated power can be converted back into energy recovered by the use of regenerative brakes or wind turbines. In this analysis we propose the recovery made by using a wind turbine.

Table 4 summarizes the results about the recovered power.

**Table 4:** Ideal percentage of power that can be recovered

	Recovery system	Recovery syst. + drag force
	Theoretical %	Theoretical %
Scenario 1	<b>21.9</b>	<b>63.45</b>
Scenario 2	<b>40.95</b>	<b>52.06</b>
Scenario 3	<b>19.73</b>	<b>78.34</b>

## 5. Conclusions

This paper is a first step to investigate the feasibility of implementing a technology for energy recovery using wind turbines in electric vehicles. This is carried out by considering the effects of the airflow through wind turbines and the vehicle aerodynamic drag during its motion. This allows to recover a percentage of the energy supplied by the batteries to the vehicle engine. Dissipative forces such as the tyre rolling resistance force are responsible for not being able to recover all the energy supplied by those batteries.

Results have shown the theoretical viability to successfully develop this technology. As important fact, this study has shown that the use of wind turbines allows the possibility of recovering an important percentage of the energy provided by the batteries, although it strongly depends on the assumptions of each case study. However, further research is needed to verify the data with experimental tests.

## References

- Bangl, V.K.T., Chaudhary, Y.; Guduru, R.K.; Aung, K.T., Reddy, G.N. (2017). Preliminary investigation on generation of electricity using micro wind turbines placed on a car. *International Journal of Renewable Energy Development*, 6(1), pp. 75-81. DOI: 10.14710/ijred.6.1.75-81.
- Ferdous, S.M, Salehin, S, Bin Khaled, W. (2011). Electric Vehicle with Charging Facility in Motion using Wind Energy. *World Renewable Energy Congress 2011 – Sweden Sustainable Transport (ST)*, 8-11 May 2011, Linköping, Sweden. DOI: 10.3384/ecp110573629.
- Llopis-Albert, C., Rubio, F., Valero, F., (2019). Fuzzy-set qualitative comparative analysis applied to the design of a network flow of automated guided vehicles for improving business productivity. *Journal of Business Research*, DOI: 10.1016/j.jbusres.2018.12.076.
- Llopis-Albert, C. Rubio, F., Valero, F. (2018). Designing Efficient Material Handling Systems Via Automated Guided Vehicles (AGVs). *Multidisciplinary Journal for Education, Social and Technological Sciences*, 5(2), 97-105. DOI: 10.4995/muse.2018.10722.
- Llopis-Albert, C., Merigó, J.M., Xu, Y.J. (2016). A coupled stochastic inverse/sharp interface seawater intrusion approach for coastal aquifers under groundwater parameter uncertainty. *Journal of Hydrology* 540, 774-783. DOI: 10.1016/j.jhydrol.2016.06.065.
- Llopis-Albert, C. Rubio, F., Valero, F. (2018a). Optimization approaches for robot trajectory planning. *Multidisciplinary Journal for Education* 5(1), 1-16. DOI: 10.4995/muse.2018.9867.
- Llopis-Albert, C., Rubio, F., Valero, F. (2015). Improving productivity using a multi-objective optimization of robotic trajectory planning. *Journal of Business Research* 68, 1429–1431. DOI: 10.1016/j.jbusres.2015.01.027.
- Llopis-Albert, C., Pulido-Velazquez, D. (2015). Using MODFLOW code to approach transient hydraulic head with a sharp-interface solution. *Hydrological processes* 29(8), 2052-2064. DOI: 10.1002/hyp.10354.
- Llopis-Albert, C., Capilla, J.E. (2010). Stochastic Simulation of Non-Gaussian 3D Conductivity Fields in a Fractured Medium with Multiple Statistical Populations: Case Study. *Journal of Hydrologic Engineering* 15(7), 554-566. DOI: 10.1061/(ASCE)HE.1943-5584.0000214.
- Rubio, F., Llopis-Albert, C., Valero, F., Besa, A.J. (2019). A new approach to the kinematic modeling of a three-dimensional car-like robot with differential drive using computational mechanics. *Advances in Mechanical Engineering*, DOI: 10.1177/1687814019825907.

-Rubio, F., Valero, F., Llopis-Albert, C. (2019a). A review of mobile robots: Concepts, methods, theoretical framework, and applications. *International Journal of Advanced Robotic Systems*, 16(2). DOI: 10.1177/1729881419839596.

-Rubio, F., Llopis-Albert, C., Valero, F., Suñer, J.L. (2016). Industrial robot efficient trajectory generation without collision through the evolution of the optimal trajectory. *Robotics and Autonomous Systems* 86, 106-112. DOI: 10.1016/j.robot.2016.09.008.

-Rubio, F., Llopis-Albert, C., Valero, F., Suñer, J.L. (2015). Assembly line productivity assessment by comparing optimization-simulation algorithms of trajectory planning for industrial robots. *Mathematical Problems in Engineering*, vol. 2015, Article ID 931048, 10 pages, 2015. <https://doi.org/10.1155/2015/931048>.

-Valero, F., Rubio, F., Llopis-Albert, C. (2019). Assessment of the Effect of Energy Consumption on Trajectory Improvement for a Car-like Robot. *Robotica*, 1-12. DOI:10.1017/S0263574719000407.

-Valero, F., Rubio, F., Llopis-Albert, C., Cuadrado, J.I. (2017). Influence of the Friction Coefficient on the Trajectory Performance for a Car-Like Robot. *Mathematical Problems in Engineering*, vol. 2017, Article ID 4562647, 9 pages. DOI: 10.1155/2017/4562647.

-Wen-Long Yao, A. and Chiu, C.-H (2015). Development of a Wind Power System on Trucks. *Universal Journal of Mechanical Engineering*, 3(5), pp. 151–163. DOI: 10.13189/ujme.2015.030501.

-Zheng, X., Lin, H., Liu, Z., Li, D., Llopis-Albert, C., Zeng, S (2018). Manufacturing Decisions and Government Subsidies for Electric Vehicles in China: A Maximal Social Welfare Perspective. *Sustainability*, 10(3), 672. DOI: 10.3390/su10030672.